JACS
JOURNAL OF THE AMERICAN CHEMICAL SOCIETY
pubs.acs.org/JACS
Article

Li vs Na: Divergent Reaction Patterns between Organolithium and Organosodium Complexes and Ligand-Catalyzed Ketone/Aldehyde Methylenation

Nathan Davison, Claire L. McMullin,* Lu Zhang, Shu-Xian Hu, Paul G. Waddell, Corinne Wills, Casey Dixon, and Erli Lu*

Cite This: J. Am. Chem. Soc. 2023, 145, 6562−6576
Read Online
ACCESS | Metrics & More | Article Recommendations | Supporting Information

ABSTRACT: Organosodium chemistry is underdeveloped compared with organolithium chemistry, and all the reported organosodium complexes exhibit similar, if not identical, reactivity patterns to their lithium counterparts. Herein, we report a rare organosodium monomeric complex, namely, [Na(CH_2SiMe_3)(Me_6Tren)] (**1**-Na) (Me_6Tren: tris[2-(dimethylamino)ethyl]amine) stabilized by a *tetra*-dentate neutral amine ligand Me_6Tren. Employing organo-carbonyl substrates (ketones, aldehydes, amides, ester), we demonstrated that **1**-Na features distinct reactivity patterns compared with its lithium counterpart, [Li(CH_2SiMe_3)(Me_6Tren)] (**1**-Li). Based on this knowledge, we further developed a ligand-catalysis strategy to conduct ketone/aldehyde methylenations, using $[NaCH_2SiMe_3]_\infty$ as the CH_2 feedstock, replacing the widely used but hazardous/expensive C═O methylenation methods, such as Wittig, Tebbe, Julia/Julia-Kocieński, Peterson, and so on.

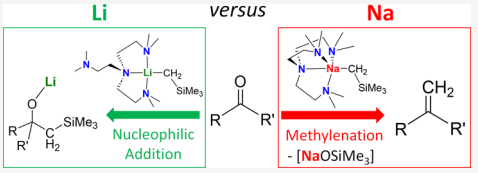

INTRODUCTION

Organosodium complexes were first reported in 1858 by James Alfred Wanklyn, describing a reaction between ethyl iodide and sodium metal.[1,2] In the following centuries, despite discrete reports of their synthesis and structures,[3−21] as well as their applications in organic,[2,22−26] inorganic,[27] and polymer[28−33] syntheses, organosodium chemistry is largely overshadowed by the dominating organolithium chemistry,[34−40] which was first reported in 1917,[34] nearly 60 years later than Wanklyn's report in 1858. The underdeveloped status of organosodium chemistry was widely attributed to the highly reactive nature and the corresponding low thermostability of these complexes.[2] The presumed low thermostability, however, is a moot point in our understanding. For example, a starting material in this work, $[NaCH_2SiMe_3]_\infty$, was found to be stable even at elevated temperature (see the Supporting Information for details).

Over 160 years after Wanklyn's inaugural report,[1] the beginning of the 2020s witnesses the renaissance of organosodium chemistry. This latest trend is largely driven by the community's efforts to seek more sustainable and economically efficient alternatives to the ubiquitous organolithium reagents. Sodium is much more abundant than lithium in the Earth's crust (Na 2.36% vs Li 0.002%[41]) and also more environmentally benign.[42] Moreover, driven by the fast rising demand of lithium-ion batteries and the unstable global geopolitical environment, the lithium price (battery-grade LiOH) has increased by 150% since the beginning of 2022 to $25,000 per metric ton, and the price is projected to further increase to $36,000 in 2023.[43] Partially motivated by these factors, since the late 2010s, synthetic chemistry community has been revisiting organosodium complexes as sustainable and economical replacement for the widely applied organolithium reagents. In 2019, Asako et al. reported that in situ formed organosodium complexes (from halogenated arenes/alkanes reacting with Na metal) served as transmetallation reagents in Pd-catalyzed cross-coupling reactions.[44,45] In a 2021 follow-up study, the same group reported a facile access to organosodium complexes via halogen-sodium exchange reactions.[46,47] In 2022, based on their previous work,[25] Knochel and co-workers reported the preparation of benzylic sodium complexes in a continuous flow setup.[48] In this case, the continuous flow technique was adopted as a countermeasure against the presumed low stability of the organosodium complexes.[25,26,48]

Nevertheless, a centuries-old paradigm in organo-alkali metal chemistry is that they may differ in activity (fast or slow reaction) and even selectivity (e.g., different deprotonation sites), yet organolithium and organosodium complexes follow the same reaction patterns. For example, they may act as Brønsted-Lowry bases, nucleophiles, transmetallation reagents (the organolithium version is Murahashi coupling[49]) or undergo halogen-metal exchange. However, for the equivalent

Received: January 30, 2023
Published: March 8, 2023

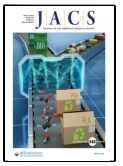

set of substrates, the organolithium and organosodium complexes have always behaved in the same pattern. Breaking the paradigm, i.e., developing strategies to tune organolithium and organosodium complexes for diversified reaction patterns, could unlock an immense unexplored chemical space and provide new sustainable and readily available tools for synthetic chemists. However, to the best of our knowledge, such a strategy is still unknown. During the preparation of this manuscript, Hevia and co-workers reported that lower aggregates of $NaCH_2SiMe_3$, which were stabilized by Lewis bases *N*,*N*,*N*′,*N*″,N″-pentamethyldiethylenetriamine (PMDTA) and tris[2-(dimethylamino)ethyl]amine (Me_6Tren), can facilitate benzylic C^{sp3}–H bond metalation and subsequent aroylation with Weinreb amides, where the corresponding organolithium complex ($LiCH_2SiMe_3$ + PMDTA) failed to deliver such reactivity.[50] It is interesting for us to note that the benzylic C^{sp3}–H bond metalation is concentration-dependent: while we reported in 2022 that the combination of $LiCH_2SiMe_3$ + Me_6Tren can deliver such metalation with neat toluene,[51] Hevia and co-workers observed that $LiCH_2SiMe_3$ + Me_6Tren/PMDTA cannot activate toluene in hexane solution.[50]

Herein, we report that a rare organosodium monomeric complex, [$Na(CH_2SiMe_3)(Me_6Tren)$] (**1**-Na), which was simultaneously reported by Hevia and co-workers,[50] exhibits distinct reactivity patterns with organic carbonyl substrates, compared with our previously reported organolithium counterpart, i.e., [$Li(CH_2SiMe_3)(Me_6Tren)$] (**1**-Li):[51] **1**-Na converts a C═O bond in ketone/aldehyde into a C═CH_2 bond, i.e., conducts ketone/aldehyde methylenation. In comparison, **1**-Li reacts with such substrates following the conventional and predictable nucleophilic addition route. Based on these observations, we designed and realized ligand-catalyzed organosodium-mediated ketone/aldehyde methylenations, providing a sustainable and easy-to-operate alternative to the classic methylenation methods (Wittig, Julia, Tebbe, Peterson, etc.). Moreover, by treating **1**-Na with amide and ester, we demonstrate the versatility of its reactivity profile, where the N- or O-substitution was found altering the reaction outcomes profoundly. These findings are elaborated in the following sections.

RESULTS AND DISCUSSION

Synthesis and Characterization of the Organosodium Monomeric Complex (1-Na). We first treated **1**-Li with one equivalent of sodium *tert*-butoxide (NaO^tBu), aimed at utilizing the NaO^tBu to activate the monomeric Li–C bond in **1**-Li and isolating a Li–Na heterobimetallic complex. Activation of polar organometallic reagents with alkali metal alkoxides is a well-documented methodology, dating back to the 1960s when the widely used LIC-KOR superbases (Lochmann–Schlosser bases) were discovered by Lochmann[52] and Schlosser.[53] The interest in this field has continued,[54] and the field was reviewed by Lochmann[55] and more recently by Mulvey and co-workers,[56] as well as by Bole and Hevia.[57] However, in our case, instead of the expected Li–Na heterobimetallic complex, we isolated **1**-Na, along with LiO^tBu (Scheme 1a). Here, a Li–Na interchange occurred.[55] Similar solubilities of **1**-Na and LiO^tBu hindered the effort to isolate these two complexes. Nevertheless, gratifyingly, pure **1**-Na was prepared from an alternative route, i.e., treating $[NaCH_2SiMe_3]_\infty$[58] with the Me_6Tren ligand, in 76% crystalline yield (Scheme 1b).

Scheme 1. Two Synthetic Routes of 1-Na[a]

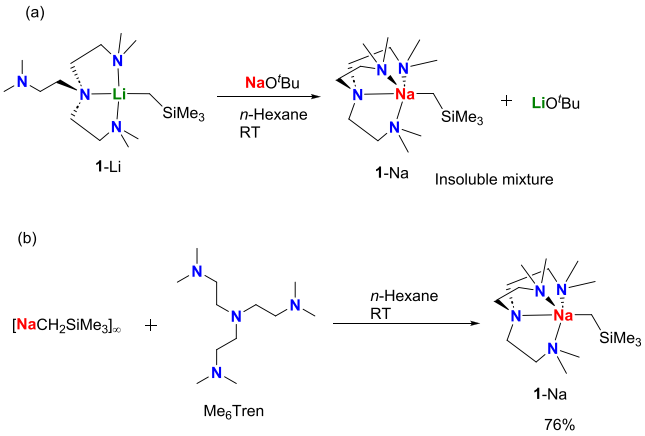

[a](a) Metal exchange between **1**-Li and NaO^tBu produces a mixture of **1**-Na and LiO^tBu. (b) Coordination between $[NaCH_2SiMe_3]_\infty$ and Me_6Tren produces clean **1**-Na.

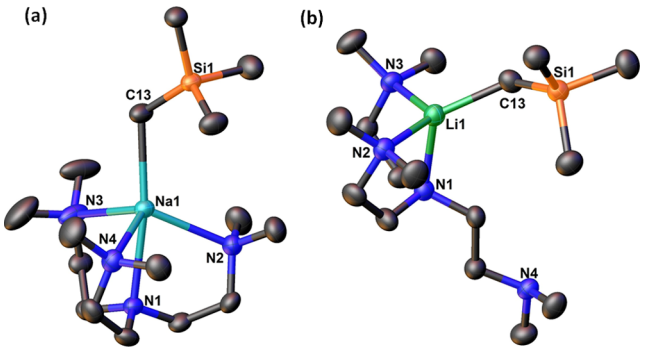

Figure 1. SCXRD structures of (a) **1**-Na and (b) **1**-Li.[51] Solvent molecules in lattice, minor disorder components, and H atoms are omitted for clarity. Representative bond lengths in comparisons between **1**-Na and **1**-Li (Å): M–C13 2.5054(14) (Na), 2.122(5) (Li); M–N1 2.6137(11) (Na), 2.177(4) (Li); M–N2 2.5232(12) (Na), 2.167(4) (Li); M–N3 2.5588(12) (Na), 2.189(4) (Li); M–N4 2.5484(13) (Na), N/A (Li).

Colorless crystals of **1**-Na suitable for single-crystal X-ray diffraction (SCXRD) analysis were obtained by storing its *n*-hexane solution at −35 °C overnight. The solid-state molecular structure of **1**-Na is shown in Figure 1a and is very similar to the structure very recently reported by Hevia and co-workers:[50] comparing the crystallographic cell parameters confirms that they are the same crystals. For comparison, the **1**-Li structure from our previous report in 2022[51] is also displayed (Figure 1b). An obvious difference between the two structures is, in **1**-Na, all the three sidearms of the Me_6Tren ligand coordinate with the Na^+ center, while in **1**-Li, only two of them coordinate. This is due to the larger ionic radius of Na^+ compared with Li^+. The Na–C and Na–N bond lengths in **1**-Na are 0.4–0.5 Å longer than the corresponding Li–C and Li–N bond lengths in **1**-Li. The proton nuclear magnetic resonance (^{1}H NMR) spectrum of **1**-Na in C_6D_6 at 298 K exhibits the typical C_3v symmetry,[59] which is consistent with its solid-state structure. Furthermore, we conducted ^{1}H diffusion ordered spectroscopy (^{1}H DOSY) studies of **1**-Na and its polymeric parent complex $[NaCH_2SiMe_3]_\infty$. **1**-Na is stable in d_{12}-cyclohexane (C_6D_{12}) at room temperature for at least 3 h with less than 30% decomposition (see SI Figure S9), allowing

https://doi.org/10.1021/jacs.3c01033
J. Am. Chem. Soc. 2023, 145, 6562–6576

Scheme 2. Initial Reactivity Studies of 1-Li and 1-Na, Employing Benzophenone (2a) as the Model Substrate[a]

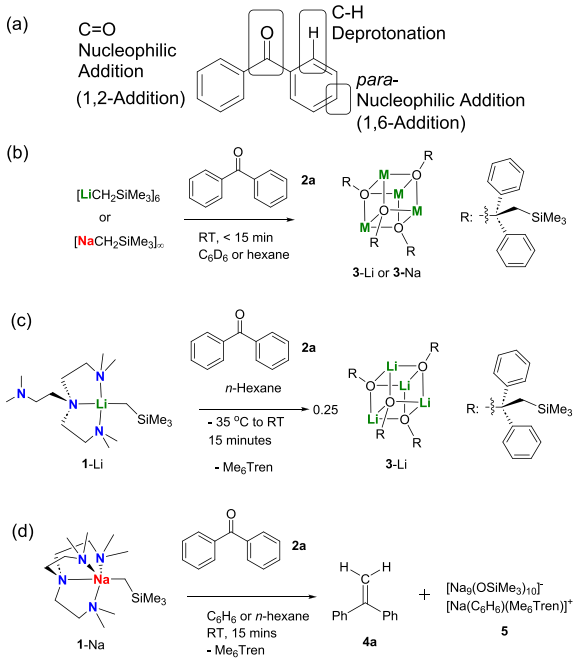

[a](a) The reactive sites of benzophenone. Stoichiometric reactions between benzophenone and (b) $[LiCH_2SiMe_3]_6$ or $[NaCH_2SiMe_3]_\infty$ and (c) **1**-Li or (d) **1**-Na.

us to study its ^{1}H DOSY spectrum. **1**-Na's molecular weight in C_6D_{12} was deduced as 333.12 (assuming expanded disc shape) or 355.57 (assuming dissipated sphere and ellipsoid shape), both are close to the actual molecular weight as a monomer (340.61) determined by SCXRD study, confirming that the solid-state monomeric structure of **1**-Na retains in solution. For comparison, the ^{1}H DOSY study of $[NaCH_2SiMe_3]_\infty$ in d_6-benzene allows us to deduce a molecular weight of 416.87 (assuming dissipated sphere and ellipsoid), indicating a tetrameric structure in solution (4 × 110.20 = 448.80). Hence, upon dissolving, the polymeric infinite structure of $[NaCH_2SiMe_3]_\infty$ breaks into tetramer $[NaCH_2SiMe_3]_4$. The Na−CH_2 ^{1}H NMR signal of **1**-Na appears at −1.42 ppm, which is comparable with the Li−CH_2 signal of **1**-Li (−1.61 ppm).[51] Natural localized molecular orbitals (NLMO) and topological analyses of the Li−C and Na−C bonds in **1**-Li/Na reveal a similar bonding scenario: both are highly ionic with the electron density mostly residing on the anionic carbon center (see SI for details).

Stoichiometric Reactions between the Li/Na Monomeric Alkyl Complexes [M(CH_2SiMe_3)(Me_6Tren)] (1-Li, 1-Na) and Ketones/Aldehydes: Nucleophilic Addition, C−H Deprotonation, or C═O Olefination? Reactions between Group-1 metal complexes and ketones/aldehydes[60] are not only important tools in organic synthesis, but also can provide insights into the two fundamental and essential reactivity aspects of Group-1 metal complexes: Brønsted basicity and nucleophilicity.[62] We first employed benzophenone (**2a**) as the model substrate to test the reactivity of **1**-Li and **1**-Na. Benzophenone was chosen as it can provide three reactive sites, covering both nucleophilic addition (1,2- and 1,6-additions[61]) and Brønsted acid−base C−H deprotonation (Scheme 2a).[62,63] Easily enolizable ketones, such as acetophenone, feature rather acidic α-Hs; hence, their reaction pattern will be predictably monopolized by the α-C−H deprotonation, i.e., enolization (vide infra).

We first tested the reactions between benzophenone and the parent polymeric/oligomeric complexes, i.e., $[LiCH_2SiMe_3]_6$ and $[NaCH_2SiMe_3]_\infty$, which unsurprisingly produced the alkoxide tetramers $[MO\{C(Ph)_2(CH_2SiMe_3)\}]_4$ (**3**-Li/Na) (Scheme 2b), the SCXRD structures of which are displayed in the Supporting Information (**3**-Na, Figure S62) or in our previous report (**3**-Li[51]). The formations of **3**-Li/Na are the result of M−C bond nucleophilic addition toward the C═O bond. Regarding the monomers, **1**-Li was reported to react with benzophenone producing **3**-Li as well, where the Me_6Tren ligand dissociates (Scheme 2c).[51] Following the

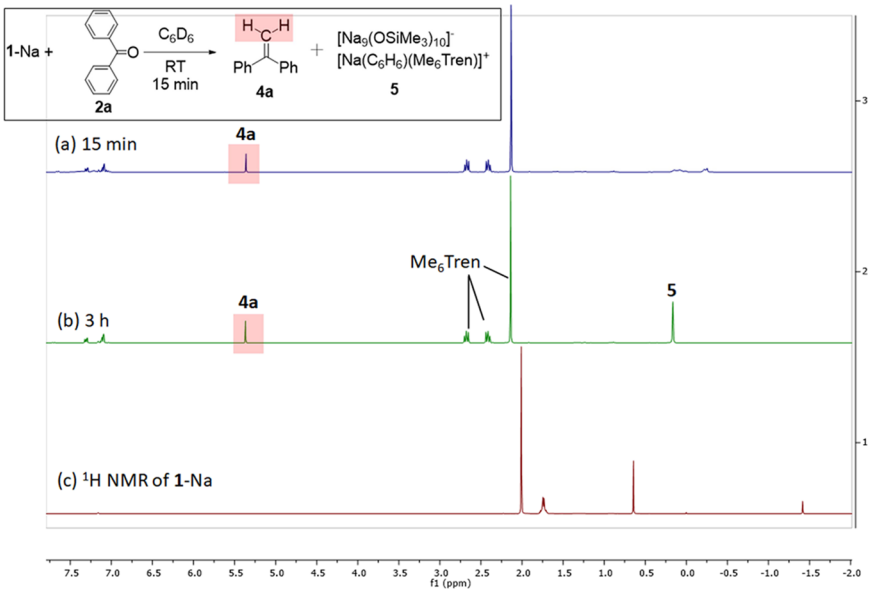

Figure 2. In situ ^{1}H NMR spectra of the reaction between **1**-Na and benzophenone **2a** (in C_6D_6, 298 K) at 15 min (a) and 3 h (b), in comparison with the ^{1}H NMR spectrum of **1**-Na (c).

https://doi.org/10.1021/jacs.3c01033
J. Am. Chem. Soc. 2023, 145, 6562−6576

Scheme 3. Johnson's Modification of Peterson Olefination, Using $[LiCH_2SiMe_3]_6$, $CeCl_3$ and Acidic/Basic Conditions[71−73]

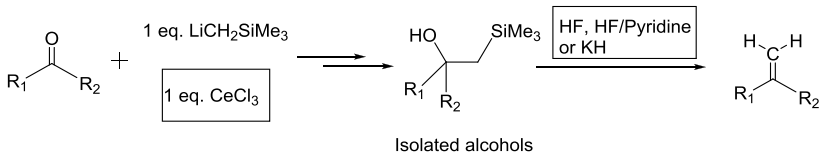

Scheme 4. Control Reactions in C_6D_6 at 60 °C[a]

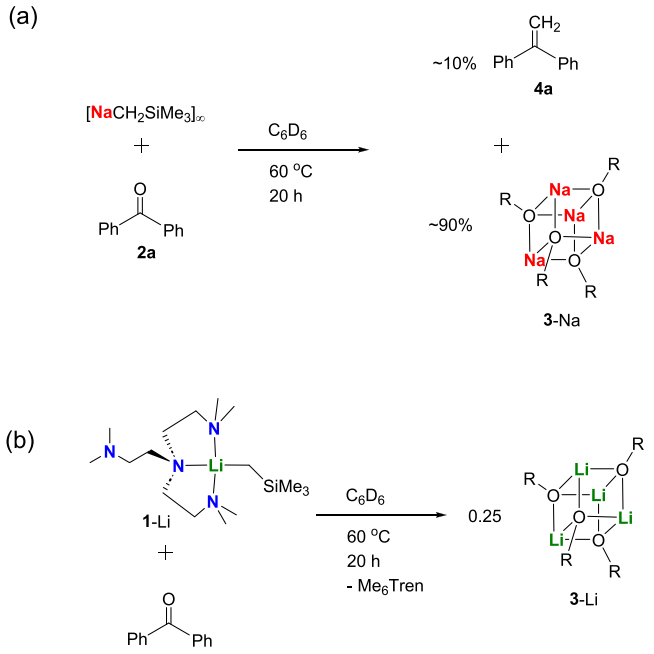

[a](a) $[NaCH_2SiMe_3]_\infty$ and benzophenone, without Me_6Tren; (b) **1**-Li and benzophenone (reported in ref 51. R: $-C(Ph_2)(CH_2SiMe_3)$.

abovementioned paradigm, one would expect that the reaction between **1**-Na and benzophenone to produce the nucleophilic addition product **3**-Na as well. However, to our surprise, instead of **3**-Na, in situ ^1H NMR spectroscopic monitoring exhibited a diagnostic singlet at 5.36 ppm within 15 min at room temperature, accompanied by a complete consumption of **1**-Na and formation of free Me_6Tren ligand (Figure 2a). The singlet, along with the aromatic Hs, is consistent with 1,1-diphenyl ethylene (**4a**) via a thorough NMR comparison (^1H, ^{13}C, DEPTs, HMQC) with the authentic sample. Another new compound **5** with a ^1H NMR singlet at approximately 0.2 ppm was formed slowly (within 3 h at room temperature) (Figure 2b). This was later identified by SCXRD study as a cluster byproduct $[Na_9(OSiMe_3)_{10}]^-[Na(C_6H_6)(Me_6Tren)]^+$ (**5**) (see Figure S61 in SI for **5**'s structure). The reaction was scaled up in benzene and *n*-hexane, which produced the same results.

The formation of **4a** involves the cleavage of a strong C−Si bond, resulting in the formation of a C═C double bond in place of the C═O bond, reminiscent of the classic methylenation by Tebbe et al.[64] and Wittig and co-workers.[65,66] In the organometallic chemistry regime, such C−Si bond cleavage in a M−CH_2SiMe_3 linkage (M: transition-metal; f-, p-, or s-block metal) is scarce but was not unknown.[67] A closely relevant class of reactions is Peterson methylenation.[68−70] For organo-alkali metal reagents, $[LiCH_2SiMe_3]_6$ has been used for Peterson methylenation since the 1980s[71] (Scheme 3), but it has to work with a stoichiometric amount of $CeCl_3$ in a stepwise manner, i.e., the intermediate alcohols must be isolated then treated with acidic/basic conditions to yield the olefins.[72,73]

We were intrigued to find out the role of the Me_6Tren ligand in the **1**-Na-mediated benzophenone methylenation. Since the free Me_6Tren ligand was observed in the in situ NMR monitoring, one may postulate that the Me_6Tren does not play any role. However, as mentioned earlier, a control reaction between $[NaCH_2SiMe_3]_\infty$ and benzophenone suggests other-

Scheme 5. Three Major Competing Reaction Patterns between 1-Na and Organic Carbonyl Substrates, and Their Corresponding Diagnostic ^1H NMR Chemical Shifts

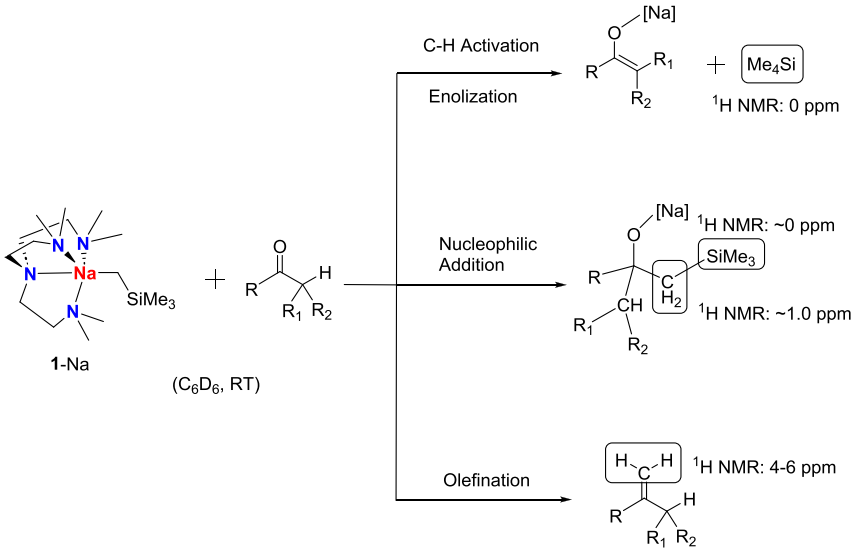

https://doi.org/10.1021/jacs.3c01033
J. Am. Chem. Soc. 2023, 145, 6562−6576

Table 1. Results of Stoichiometric Reactions between 1-Na and Ketones/Aldehydes

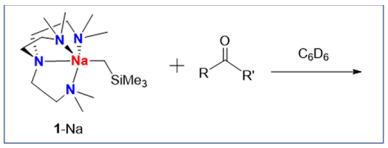

	condition		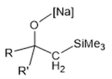		color codes for dominating reaction pattern
 2a	RT, 15 min	<5%	<5%	>95%	methylenation
 2b	RT, 15 min	>95%	<5%	<5%	deprotonation
 2c	RT, 30 min	~30%	<5%	~70%	nucleophilic addition
 2d	RT, 30 min	<5%	<5%	>95%	intractable mixture
 2e	RT, 30 min	<5%	<5%	>95%	
 2f	RT, 30 min	<5%	<5%	>95%	
 2g	RT, 3 h	n/a	>95%	<5%	
	RT, 3 days	n/a	<5%	>95%	
 2h	RT, 30 min	n/a	<5%	>95%	
 2i	RT, 2 h	n/a	<5%	>90%	
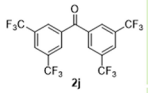 2j	RT, 30 min	n/a	<5%	>90%	
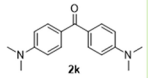 2k	RT, 18 h	n/a	<5%	>95%	
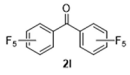 2l	RT, 30 min	intractable mixture			

wise (Scheme 4a). In the absence of Me_6Tren, **3**-Na was the major product with only small amount (~10%) of the olefin **4a**, even at an elevated temperature (60 °C) for an extended reaction time (20 h) (Scheme 4a). Hence, clearly, although Me_6Tren appears as coordination-free, it does play an essential role in the methylenation. Another key factor is metal identity. The control reaction between **1**-Li and benzophenone (Scheme 4b) produced **3**-Li and free Me_6Tren.[51] Despite the presence of one equivalent of Me_6Tren, **3**-Li does not convert into the olefin **4a** at all, even after heating at 60 °C for 20 h. Therefore, it is clear that two factors play underpinning roles in the benzophenone methylenation: (1) Me_6Tren ligand must be present; (2) Na^+ is essential.

Encouraged by the facile benzophenone methylenation, we examined stoichiometric reactions between **1**-Na and various hydrocarbon and fluorinated ketones and aldehydes. We anticipate three major competing reaction patterns (Scheme 5): (1) C−H deprotonation to form enolates (enolization), (2) nucleophilic addition to form alkoxides, and (3) methylenation. The competing reaction patterns were monitored at the NMR scale by their corresponding characteristic ^{1}H NMR chemical shifts (Scheme 5).

The results are listed in Table 1. For the easily enolizable ketone acetophenone (**2b**), enolization was observed exclusively. For less enolizable ketones, such as dicyclohexyl ketone (**2c**) and phenyl cyclohexyl ketone (**2d**), methylenation was observed as the dominating reaction pattern. Non-enolizable ketones, such as phenyl *tert*-butyl ketone (**2e**) and adamantanone (**2f**), were observed to undergo methylenation as well. Though slower than the ketones, the methylenation also works for aldehydes (**2g**, **2h**). On the course of the conversion from benzaldehyde (**2g**) to styrene (**4g**), we observed the nucleophilic addition product as the intermediate.[59] Hence, it is sensible to postulate that, with the presence of Me_6Tren, the nucleophilic addition product undergoes methylenation. The long methylenation time (3 days) for **2g**

https://doi.org/10.1021/jacs.3c01033
J. Am. Chem. Soc. 2023, 145, 6562−6576

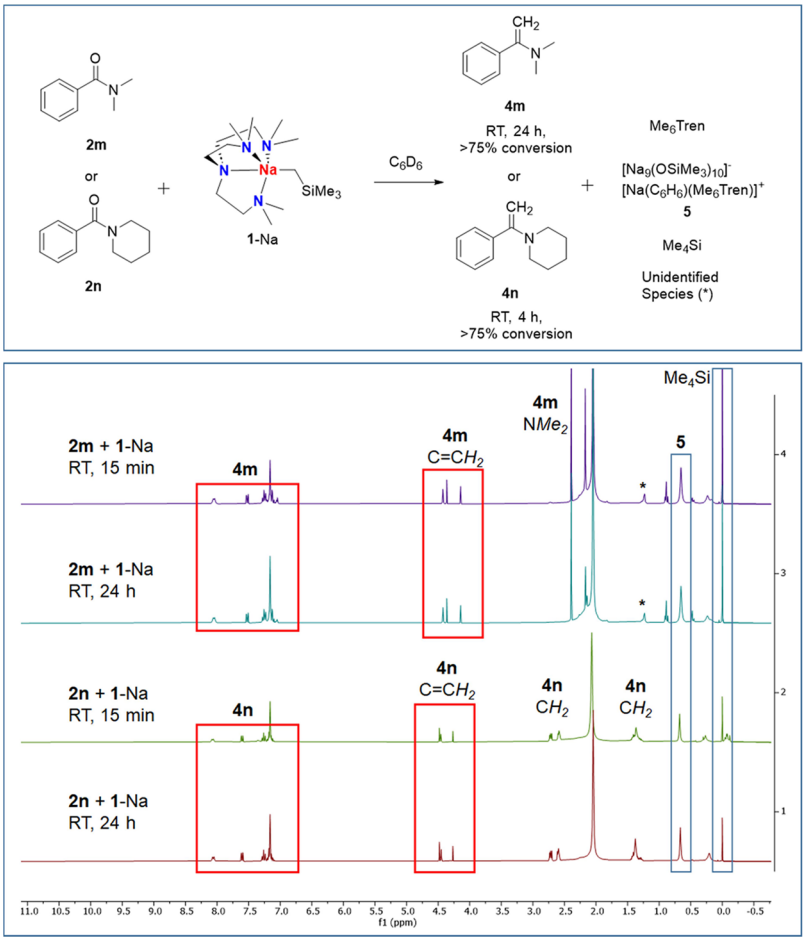

Figure 3. In situ ^{1}H NMR spectra of the reactions between **1**-Na and *N*,*N*-dimethylbenzamide (**2m**) or 1-benzoylpiperidine (**2n**) (in C_6D_6, 298 K).

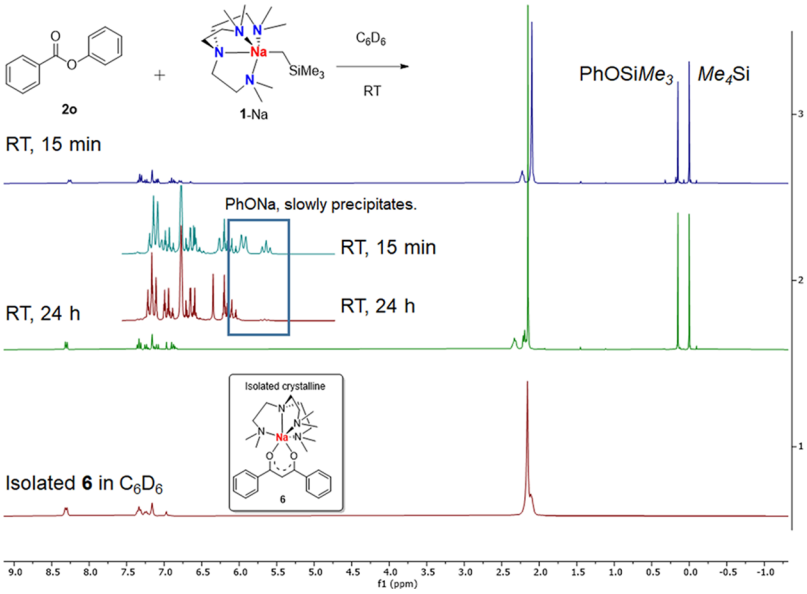

Figure 4. In situ ^{1}H NMR spectra of the reaction between **1**-Na and phenyl benzoate **2o** and ^{1}H NMR spectrum of isolated crystalline **6** (all in C_6D_6, 298 K).

can be explained by its more stable nucleophilic addition product as a result of its reduced steric congestion compared with the ketones. In comparison, the methylenation of a bulkier aldehyde **2h** is much faster (room temperature, 30 min). We postulate that the steric factor plays a crucial role here: **1**-Na-mediated methylenation prefers bulkier substrates, because their corresponding nucleophilic addition products (alkoxides) are less stable. The preference of sterically bulky substrates is in sharp contrast with the classic Wittig/Tebbe

https://doi.org/10.1021/jacs.3c01033
J. Am. Chem. Soc. 2023, 145, 6562−6576

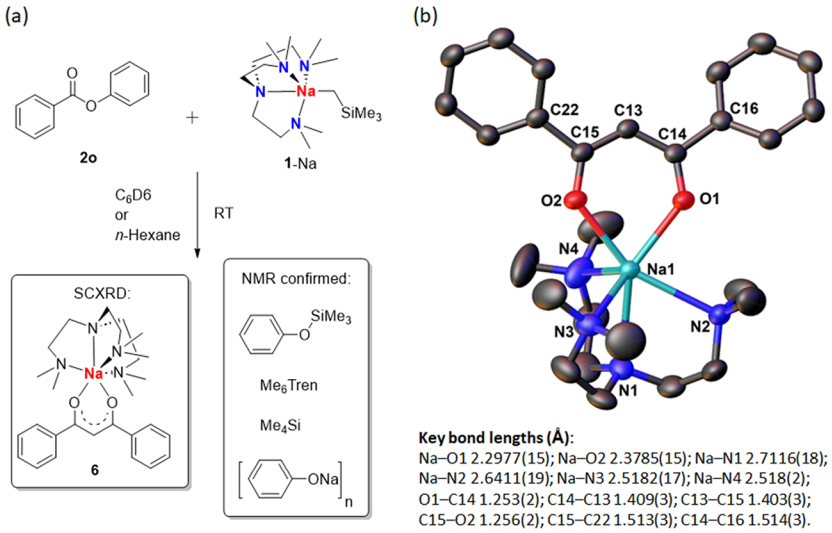

Figure 5. (a) Reaction between **1**-Na and ester **2o**; (b) SCXRD structure of **6**; H atoms are omitted for clarity.

Scheme 6. Postulated Mechanism of the Reaction between 1-Na and 2n[a]

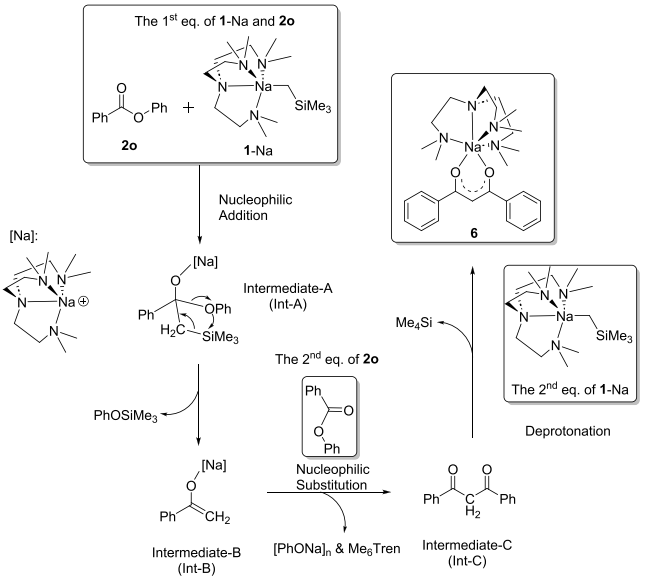

[a]The postulated reaction intermediates are identified as Int-A, Int-B, and Int-C.

systems, which operate via a crowded 2 + 2 cycloaddition transition state, hence favoring less bulky substrates.

Beyond the hydrocarbon ketones and aldehydes, we also tested reactions between **1**-Na and ketones with strong electron-withdrawing or electron-donating groups, to examine the influence of C═O bond electronic properties. Reactions between **1**-Na and electron-poor fluorinated ketones, namely, 2,2,2-trifluoroacetophenone (**2i**) and 3,3′,5,5′-tetrakis-(trifluoromethyl)benzophenone (**2j**), both produce methylenation products smoothly (Table 1). The electron-rich 4,4′-bis(*N*,*N*-dimethylamino)benzophenone (Michler's ketone,[74] **2k**) also reacts with **1**-Na to produce the methylenation product. However, perfluorobenzophenone (**2l**) reacts with **1**-Na to produce an intractable mixture, without observable formation of the corresponding olefin, nor the nucleophilic addition product. We attribute the negative result with **2l** to its highly electron-deficient perfluorophenyl groups, which are labile to nucleophilic substitution.[75,76] Since s-block metal alkyl complexes were reported to undergo nucleophilic substitution with arenes such as benzene,[77,78] it is sensible to postulate that the Na−C bond in **1**-Na, which is rather nucleophilic, reacts with the electron-deficient $-C_6F_5$ group in **2l** following a nucleophilic route.

Stoichiometric Reactions between [Na(CH_2SiMe_3)-(Me_6Tren)] (1-Na) and Ester or Amide: O vs N. Group-1 and 2 metal alkyl complexes were reported to undergo a variety of reactions toward organic amides and esters, spanning from conventional nucleophilic addition[79−82] and substitution,[83,84] to less common reductive coupling (in the presence of an redox-active iron cluster).[85] From an electronic perspective, in esters and amides, there is pronounced electron density donation from the lone pair of N/O atoms to the carbon atom of C═O bonds, which renders the C═O bond less electrophilic compared with ketone/aldehyde, i.e., less labile to nucleophilic addition. This was clearly demonstrated by Beak and Brown as early as in 1982, where the amide functional group acted as a directing group for organolithium-mediated arene *ortho*-lithiation,[86] where phenyl ring deprotonation occurred, instead of amide nucleophilic addition. Considering the versatile reactivity profile of ester/amide, we were intrigued to examine their reaction patterns with our organosodium monomer complex **1**-Na.

N,*N*-Dimethylbenzamide (**2m**), 1-benzoylpiperidine (**2n**), and phenyl benzoate (**2o**) were employed as readily available and representative model substrates. Reactions between the amides **2m**/**2n** and one equivalent of **1**-Na in C_6D_6 proceeded predominantly toward methylenation (over 75% conversion calculated from ^{1}H NMR) at room temperature within 24 h (for **4m**) or 4 h (for **4n**), respectively (Figure 3). A small amount of Me_4Si was observed in both **4m** and **4n** reactions (circa 15−20%), indicating deprotonation side-reactions, which are not surprising considering the Brønsted acidity of the $N(CH_3)_2$ (**2m**) and NCH_2 (**2n**) groups.

However, reaction between phenyl benzoate (**2o**) and one equivalent of **1**-Na in C_6D_6 did not produce the methylenation product, judging from the lack of the diagnostic olefin C^{sp2}−*H* signals in its ^{1}H NMR spectrum (Figure 4). Instead, Me_4Si, $PhOSiMe_3$[87] and sodium phenoxide $[PhONa]_n$ were identified

https://doi.org/10.1021/jacs.3c01033
J. Am. Chem. Soc. 2023, 145, 6562−6576

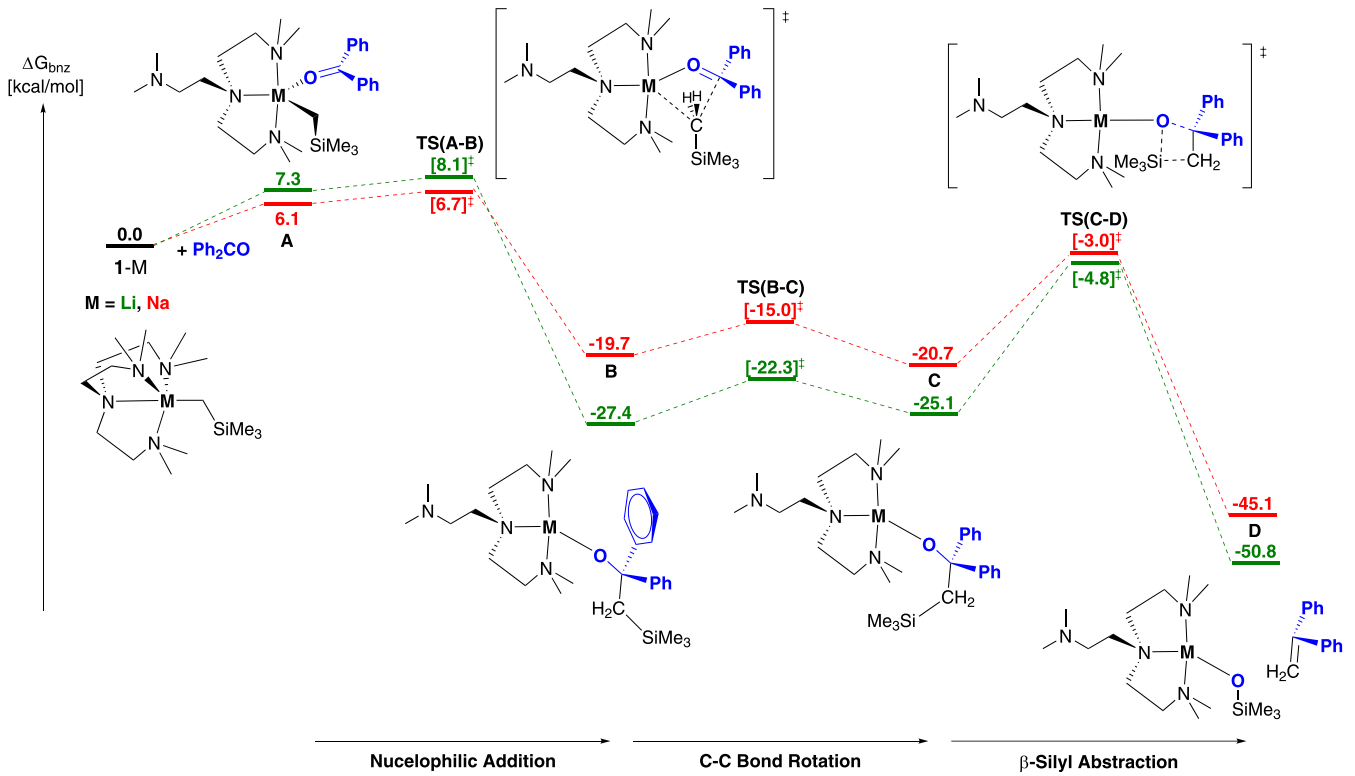

Figure 6. DFT-calculated free energy profile (BP86-D3BJ(C_6H_6)/6-311++G**//BP86/6-31G**&SDDALL, in kcal mol^{-1}) for the reaction of **1**-M (M = Li, Na) with benzophenone (in blue). Calculated intermediates are named as **A**, **B**, and **C**, while the calculated Me_6Tren-chelated silyloxide product is **D**. Color codes for the reaction pathways: Li = green pathway, Na = red pathway.

(Figure 4). Scaling up the reaction and crystallization in *n*-hexane at −35 °C afforded yellow needle-shaped crystals at low but reproducible yield (approximately 17% based on Na), the structure of which was characterized as an Me_6Tren-coordinated sodium phenyl-acetylacetonate complex **6** (Figure 5). Coordination-free Me_6Tren was recovered from the mother liquor of crystallization.

The outcome of the reaction between **1**-Na and **2o** is surprising, involving cleavage of C−O bonds and formation of O−Si and C−C/C═C bonds. As a net result, two [PhC(O)] units (originated from the ester **2o**) are linked by a [CH] unit. We hypothesized that the [CH] unit is from [$NaCH_2SiMe_3$]. To the best of our knowledge, this reaction pattern is hitherto unknown for esters. The formations of $PhOSiMe_3$ and Me_4Si provide crucial clues, allowing us to postulate a sensible reaction mechanism to explain the outcome (Scheme 6): The reaction is initiated by a nucleophilic addition of the Na−C bond toward the C═O bond, followed by an intramolecular $PhOSiMe_3$ elimination, driven by the formation of a strong O−Si bond. The resultant enolate intermediate underwent a nucleophilic substitution with the second equivalent of **2o** and eliminated $[PhONa]_n$ and free Me_6Tren ligand. Subsequently, the resultant 1,3-diphenyl-1,3-propanedione (Int-C in Scheme 6) is deprotonated by the second equivalent of **1**-Na to produce **6** and Me_4Si.

We rationalize the dramatically different reaction patterns between the amides **2m**/**2n** and ester **2o** by the key step of intramolecular $PhESiMe_3$ (E: O, N) elimination (Int-A in Scheme 6): the formation of a relatively weak N−Si bond (bond dissociation energy (BDE) 493 kJ mol^{-1}) is less favorable than a strong O−Si bond (BDE 798 kJ mol^{-1}).[88] Though we believe that the postulated reaction mechanism in Scheme 6 is sensible, it should not be treated as a calculated reaction pathway analysis, which is currently underway in our groups, along with further effort to expand the ester/amide substrate scopes for exploiting the new reactivity. These results will be published in due course as follow-ups of the initial discovery presented herein.

Li vs Na, Nucleophilic Addition vs Methylenation: Probing the Origin of the Diversified Reaction Patterns Using Density Functional Theory (DFT) Calculations—A Case Study of Benzophenone (2a). To gain insight into the different reactivity observed in this reaction system, DFT calculations first looked at the **1**-M (M = Li, Na) species, and in particular the coordination mode of the Me_6Tren ligand. Using a dispersion and solvation corrected methodology (see the SI for full details), the κ^4 coordination mode, where all three sidearms of the Me_6Tren ligand are coordinated to the metal center, is preferred for both Na and Li, by 6.6 and 3.3 kcal mol^{-1} respectively, compared to the κ^3/two sidearms coordinated conformer. Natural charges show little differentiation between the metal centers (q_M = 0.81−0.83) or the directly coordinated carbon atom (q_C = −1.53 − −1.58) of the CH_2SiMe_3 fragment for both conformers (see the SI), suggesting that the electronics of the starting complex does not influence reactivity. The stability of the tetrameric alkoxide product **3**-M (M = Li, Na) was also explored, with exergonic cluster formation being preferred for M = Li by 19.5 kcal mol^{-1} in comparison to M = Na, with an overall free energy of formation of −142.5 kcal mol^{-1} for **3**-Li.

Reaction profiles were modeled for both **1**-Na and **1′**-Li (the hypothetic κ^4 version of **1**-Li), with and without Me_6Tren coordination, and for no Group-1 metal involvement, with the relative zero species being either **1**-Na or **1′**-Li, both the κ^4

https://doi.org/10.1021/jacs.3c01033
J. Am. Chem. Soc. 2023, 145, 6562−6576

Table 2. Me_6Tren-Catalyzed Ketone/Aldehyde Methylenation Mediated by $[NaCH_2SiMe_3]_\infty$ and Corresponding Control Reactions with the Conversions Measured by ^{1}H NMR (See the Supporting Information for Details)

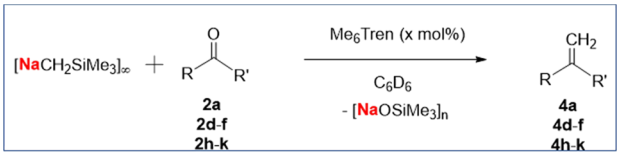

entry	substrate	Me_6Tren mol%	temp. & time	conversion	product	control reaction (No Me_6Tren) (conversion %)
1	 2a	20%	RT, 3 h	>95%	 4a	60 °C, 20 h <10%
2		5%	RT, 16 h	>95%		
3	 2d	5%	RT, 2 h	>95%	 4d	RT, 3 h <5%
4	 2e	5%	RT, 2 h	>95%	 4e	RT, 3 h ~25%
5	 2f	5%	RT, 2 h	>95%	 4f	RT, 3 h ~10%
6	 2h	5%	60 °C, 15 h	>95%	 4h	60 °C, 18 h <5%
7	 2i	5%	RT, 3 days	>95%	 4i	RT, 3 days <5%
8	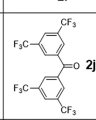 2j	5%	RT, 3 days	>75%	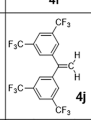 4j	RT, 3 days <5%
9	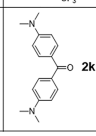 2k	5%	60 °C, 16 h	>95%	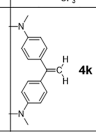 4k	60 °C, 16 h <5%

species (Figure 6). The first step of the reaction profiles requires endergonic coordination of **2a** (benzophenone) to the metal after dissociation of one of the N sidearms (to the κ^3 conformer). This is easier for the sodium system, with intermediate **A**-Na 6.1 kcal mol^{-1} higher in free energy than **1**-Na. Similarly, the more sterically crowded (due to the smaller ionic radius of Li^+) **A**-Li was eventually optimized and found to be 7.3 kcal mol^{-1} higher in free energy than **1′**-Li, see Figure 6. Nucleophilic addition (**TS(A-B)**) of the silyl alkyl group to the carbonyl carbon proceeds irreversibly by a barrier of 0.6 (**A**-Na) and 0.8 (**A**-Li) kcal mol^{-1}, relieving the steric strain of the five coordinate metal center, to give the exergonic intermediate **B**, where the alkoxide is bound to the metal through the oxygen of **2a** and the $SiMe_3$ group in an *anti*-conformation (O−C−C−Si dihedral close to 180°).

Subsequent low barriers (4.7 (**B**-Na) and 5.1 (**B**-Li) kcal mol^{-1}) to C−C bond rotation (**TS(B-C)**) of the newly formed bond ensure that the $SiMe_3$ group moves to a *syn* conformation (**C**), with a O−C−C−Si dihedral value close to 0°. Here, the intermediate is now primed for the following β-silyl abstraction, where the oxophilic trimethylsilyl is abstracted by the negatively charged oxo, involving simultaneous O−C and C−Si cleavage as further overlap occurs between the carbon centers to form the olefinic C=C π bond. This concerted β-silyl abstraction process was located via a four-membered transition structure **TS(C-D)**, which resembles a 1,2-oxasiletanide reported by Okazaki and co-workers in 1992,[89] and is rate limiting for both the Na and Li ligated systems, with barriers of 17.2 and 22.5 kcal mol^{-1} found at −3.0 and −4.8 kcal mol^{-1} for **C**-Na and **C**-Li respectively. The higher barrier of **C**-Li could determine that the reaction does not proceed for the Li system, as experimentally observed. This then affords the olefin product adduct, **D**, which is irreversibly and exergonically formed at −45.1 kcal mol^{-1} for **D**-Na (−50.8 kcal mol^{-1} for **D**-Li).

In the absence of the Me_6Tren ligand, reaction profiles were also computed for **2a** reacting with $[CH_2SiMe_3]^-$ in the presence of one atom of Na or Li (see the Supporting Information Figure S67 for Na and Figure S68 for Li, respectively). Coordination of **2a** to M(CH_2SiMe_3) raised the free energy of ^{M}**A** to over 16 kcal mol^{-1} followed by nucleophilic addition at 23.5 and 21.4 kcal mol^{-1}, for M = Na and Li, respectively. Without the ligand to support the electron density on the metal, the nucleophilic addition barriers are larger by 8.2 and 5.3 kcal mol^{-1}. Subsequent rotation about the new C−C bond, **TS(B-C)**, has a free energy barrier of 6.9 kcal mol^{-1} for Na (Li = 6.7 kcal mol^{-1}), now larger due to a π-interaction between the metal and a phenyl ring of **2a**. The 1,2-oxasiletanide transition state, **TS(C-D)**, occurs at 15.9 kcal mol^{-1} (Li = 19.5 kcal mol^{-1}). Again, β-silyl abstraction and olefin formation were notably easier for the Na system by 4.5 kcal mol^{-1}, compared to 5.3 kcal mol^{-1} with the ligated systems. Hence, we conclude that ligation is the key to a lower barrier for nucleophilic addition. This explains the necessity of the Me_6Tren ligand to facilitate the methylenation.

In the absence of a metal (Figure S69), the adduct **a** is substantially higher in free energy at 32.5 kcal mol^{-1} with the system balanced by the separated ion pair complex [(κ^4-Me_6Tren)Na]. The equivalent nucleophilic addition transition structure, **TS(a-b)**, has a barrier of 1.9 kcal mol^{-1}, to form the *anti*-alkoxide conformer, **b**, at 15.9 kcal mol^{-1}. Rotation about the C−C bond has two distinct barriers, **TS(b-c)1** and **TS(b-c)2** both under 2 kcal mol^{-1}, and an intermediate **INT(b-c)**, before the *syn* conformer is isolated as **c** at 9.1 kcal mol^{-1}. The final β-silyl abstraction step, **TS(c-d)**, was optimized at 21.5 kcal mol^{-1}.

The calculated reaction pathways in Figure 6 clearly demonstrate that **1**-Na and **1′**-Li could both react with **2a** (benzophenone) and follow a similar reaction pathway. However, while the methylenation with **1**-Na proceeds at room temperature rapidly, the corresponding methylenation with **1**-Li was not experimentally observed, even at elevated temperature (60 °C). We note that, in Figure 6, the energetic barriers are consistently higher for **1′**-Li than those for **1**-Na. This could be one contributor for not observing methylenation with the Li system. However, we caution using the higher barriers of **1′**-Li as the sole explanation: the energetic differences between the barriers for **1′**-Li and **1**-Na are small (maximum 5.3 kcal mol^{-1}, for **TS(C-D)**). Another potential contributor is steric, i.e., the larger Na^+ ionic radius may favor methylenation. To summarize, we hypothesize that the observed difference between **1**-Na and **1**-Li methylenation could be a result of interplay among several factors, including a series of slightly higher energetic barriers for the Li system, and the more favorable steric factor endowed by the larger Na^+ cation. Though a definite answer is absent for now, these

https://doi.org/10.1021/jacs.3c01033
J. Am. Chem. Soc. 2023, 145, 6562−6576

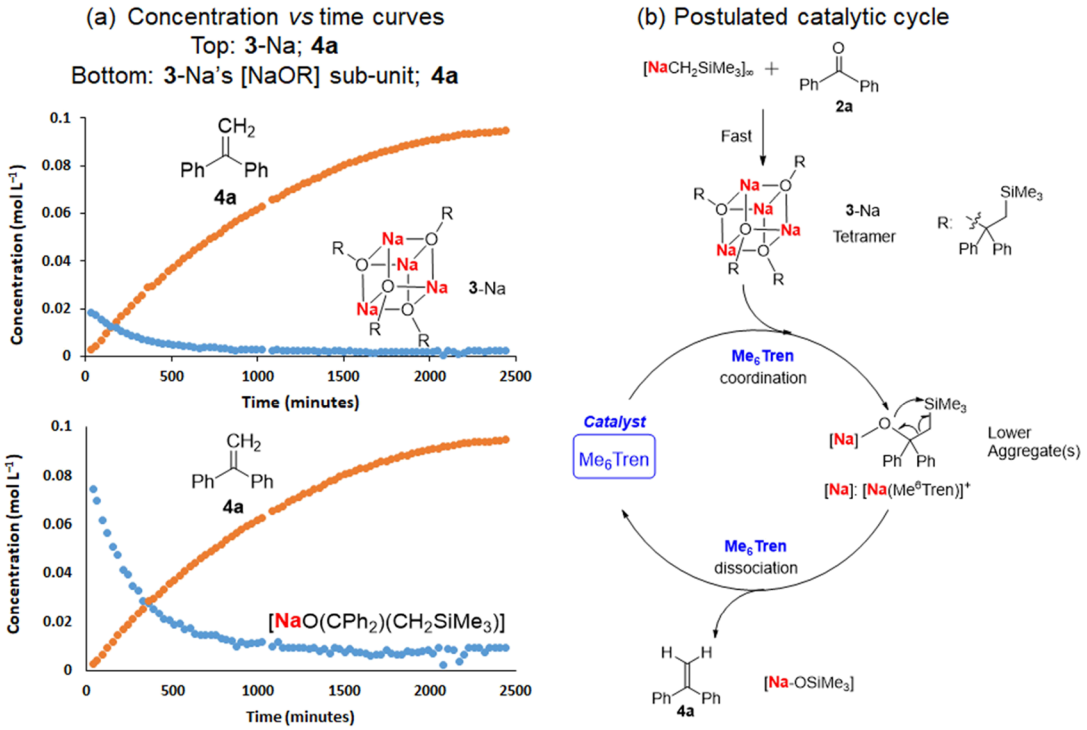

Figure 7. In situ ^{1}H NMR monitoring of catalyzed benzophenone methylenation and its postulated mechanism. (a) Concentration *vs* time curves. Catalytic conditions: room temperature, C_6D_6, 5 mol % of Me_6Tren, initial substrate concentration $[\mathbf{2a}]_0$ = 0.08 M; catalyst concentration $[Me_6Tren]$ = 0.004 M; internal standard: cyclohexane. For full details, see Supporting Information, Section 1.6, page S41. (b) Postulated catalytic cycle.

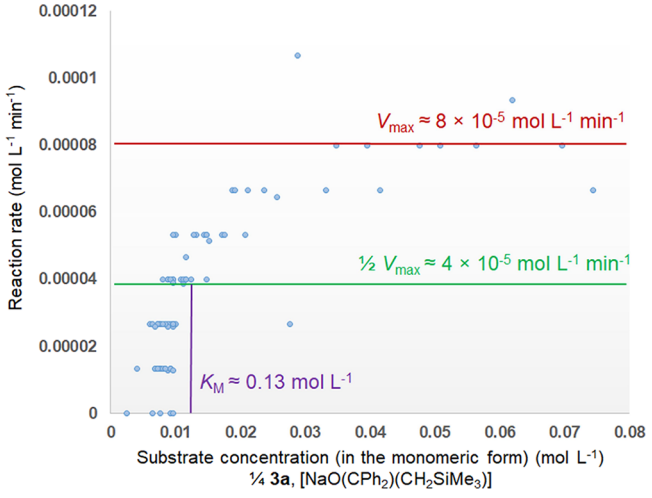

Figure 8. Michaelis–Menten saturation plotting (reaction rate-substrate concentration) for 5 mol % Me_6Tren-catalyzed methylenation of benzophenone (**2a**) with $NaCH_2SiMe_3$. The solid lines for V_{max}, 1/2 V_{max}, and K_M are for visual guide only. The analyses represented herein should be treated as qualitative, rather than quantitative.

calculations clearly demonstrate that organo-alkali metal reactions involve delicate balances: changing metal identity could shift the finely-balanced pathway, and result in a dramatic change of reaction outcomes, though the energetic changes of each single step may appear trivial.

Our argument can be supported by a study on amino-metalations by Strohmann and co-workers,[90] where they calculated the reaction profiles between lithium-, sodium- and potassium dimethylamide dimers $[M(\mu\text{-}NMe_2)(OMe_2)_n]_2$ and 4-methyloxy styrene. The scenario is similar to our case in Figure 6 but with larger energetic differences. Nevertheless, unlike we observed here, Strohmann and co-workers did not experimentally observe different reaction patterns between the Li-, Na-, and K-amides per se. They alternated the balances by adding the second Group-1 metal ingredient to form the Lochmann–Schlosser-type heterometallic systems, which operates in a totally different mechanism. In comparison, in our system here, the difference between the metal identity itself (Li vs Na) is pronounced enough to result in divergent reaction patterns.

Ligand-Catalyzed Organosodium-Mediated Ketone/Aldehyde Methylenation. Inspired by the presence of the coordination-free Me_6Tren in the olefination of benzophenone, we wondered if a catalytic amount of Me_6Tren would promote the methylenation, employing $[NaCH_2SiMe_3]_\infty$ as the stoichiometric CH_2 transfer reagent. Compared with other popular CH_2 transfer reagents, such as phosphorus ylides (Wittig[91]), sulfones (Julia[92] and Kocieński[93]), titanium (Tebbe[64]), zirconium,[94] rare-earth,[95] molybdenum (Kauffmann[96]), or chromium (Takai[97]) reagents, the organosodium reagent $[NaCH_2SiMe_3]_\infty$ features significant sustainability advantages and, potentially, a much lower cost (for comparison, Tebbe reagent solution (0.5 M in toluene) is priced at £229 for 25 mL at Merck). The concept of ligand-catalysis (and the relevant solvent-catalysis[98]) is based on reversible coordination of a ligand (e.g., Me_6Tren in this case) to the metal center, which has been seldom reported in Group-1 metal chemistry as early as in the 1960s[99−101] until today,[102−104] mostly for deprotonation reactions.

By using 20 mol % of Me_6Tren as a catalyst, the 1:1 reaction between $[NaCH_2SiMe_3]_\infty$ and benzophenone yielded the olefin **4a** in >95% conversion within 3 h at room temperature

https://doi.org/10.1021/jacs.3c01033
J. Am. Chem. Soc. 2023, 145, 6562−6576

(Table 2, entry 1). Lowering the catalyst loading to 5 mol % worked well, too; despite the longer reaction time (16 h, room temperature) needed to reach >95% conversion (Table 2, entry 2). In situ ^{1}H NMR monitoring of the 5% Me_6Tren-catalyzed benzophenone methylenation reveals that it is a stepwise reaction. First, benzophenone was fully and rapidly converted into the alkoxide tetramer **3**-Na within 10 min at room temperature, this then slowly converted into the olefin **4a** (Figure 7a). The concentration vs time curves of **3**-Na's consumption and **4a**'s formation are presented in Figure 7a. It should be noted that **3**-Na is a tetramer (Figure 7a top). For clarity, the following discussion will use the concentration of its monomeric subunit [NaOR] (Figure 7a bottom), which is higher than the concentration of **3**-Na itself and hence, elucidates the trend more clearly. It can be observed that the consumption of [NaOR] and the formation of **4a** follow different trends (Figure 7a bottom). At the initial stage of reaction (0 to ∼300 min), [NaOR] is rapidly consumed, but **4a** only rises slowly. This indicates the presence of intermediate(s), which we identified on the ^{1}H NMR (see the Supporting Information Figure S56, highlighted in pink band) and postulate to be lower aggregate(s) of **3**-Na. Hence, we postulate a catalyzed reaction mechanism as depicted in Figure 7b: $[NaCH_2SiMe_3]_\infty$ rapidly reacts with benzophenone in a nucleophilic addition manner to form **3**-Na (a tetramer), which is subsequently slowly dissembled by the catalytic amount of Me_6Tren into lower aggregate(s) intermediate(s), which then undergoes fast methylenation and regenerates the ligand catalyst Me_6Tren. The lower aggregate(s) play an important role in our hypothesis but due to their low concentration and fast conversion into the methylenation product, we could not experimentally identify them unambiguously.

To gain further insight into the catalytic process, we adopted the Michaelis–Menten (M–M) method[105] to analyze the kinetic data of 5 mol % Me_6Tren-catalyzed benzophenone methylenation. By adopting the M–M method, we hypothesize that the Me_6Tren in our system plays the role of enzyme in the classic M–M model. The average reaction rate at each time point (t_n) was calculated by dividing the increase of product concentration (in mol L^{-1}; $\Delta[\mathbf{4a}] = [\mathbf{4a}]_n - [\mathbf{4a}]_{n-1}$; n = 1, 2, 3...; $[\mathbf{4a}]_0$ = 0 mmol L^{-1}) by time length (in minute; $\Delta t = t_n - t_{n-1}$), i.e., $d[\mathbf{4a}]/dt$, in the unit of mol L^{-1} min^{-1}. A resultant reaction rate-substrate concentration plotting (Michaelis–Menten saturation plotting) is displayed in Figure 8. The key parameter of our interest is the Michaelis constant, K_M, which is defined as the substrate concentration when the reaction rate is half of the maximum rate V_{max}. In the classic M–M model, K_M is a probe for the enzyme's affinity to substrate: a small K_M indicates high enzyme-substrate affinity, i.e., the reaction rate will approach V_{max} at lower substrate concentration.[106] Examining Figure 8 indicates that, though a quantitative understanding of the system is out of our reach at the moment (largely due to lack of accurate reaction rate data), qualitatively speaking, our system features a relatively small K_M (circa 0.13 mol L^{-1}), which indicates a strong affinity between Me_6Tren and the $[NaO(CPh_2)(CH_2SiMe_3)]_n$ species.

Encouraged by the success of benzophenone, we subsequently expanded the catalytic substrate scope to **2d–f** and **2h–k**, all of which exhibited good to excellent catalytic activities (Table 2, Entries 3–9). For **2d–f**, 5 mol % of Me_6Tren catalyzed their methylenations within 2 h at room temperature with >95% conversion. The catalytic methylenation of 9-anthracenealdehyde (**2h**) is slower (15 h) and requires an elevated temperature (60 °C) to achieve >95% conversion. The fluorinated (**2i**, **2j**) and electron-rich (**2k**) ketones all need longer reaction times or higher temperature to achieve high conversions, too.

CONCLUSIONS AND OUTLOOK

In conclusion, in this work we reported several new discoveries that push forward the frontiers of organosodium, and more generally, organo-alkali metal chemistry. First, we reported the first unequivocal observation of divergent reaction patterns between organolithium and organosodium reagents, with a variety of ketone/aldehyde substrates (Figure 9a). Second, we clearly demonstrated different reaction patterns of the $NaCH_2SiMe_3$ monomer (**1**-Na) and polymer ($[NaCH_2SiMe_3]_\infty$) toward model ketone substrate: benzophenone (Figure 9b). Beyond ketones and aldehydes, **1**-Na was found to react with amide and ester via different pathways, which further demonstrated the hitherto unexplored versatile reactivity of organosodium complexes. Based on the stoichiometric reactivity studies, we pushed the organosodium-mediated ketone/aldehyde methylenations into the catalysis regime and developed a ligand-catalysis strategy,

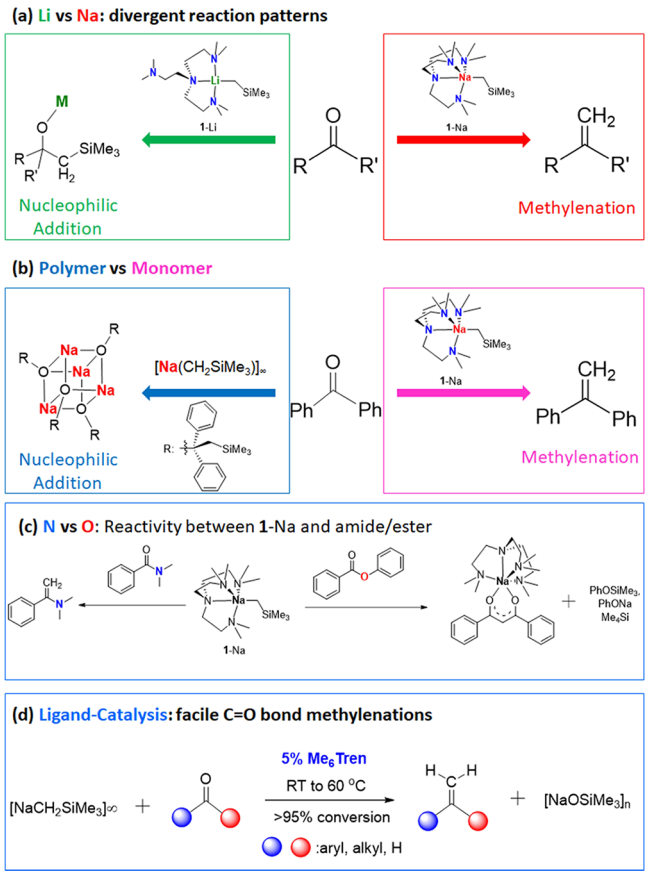

Figure 9. Schematic summary of the work herein. (a) Divergent reaction patterns between organosodium and organolithium complexes toward ketone/aldehyde; (b) diversified reactivity of organosodium complexes: polymer vs monomer; (c) diversified reactivity of **1**-Na toward amide/ester; (d) ligand-catalyzed C=O bond methylenation using organosodium reagent as a sustainable and low-cost CH_2 feedstock.

https://doi.org/10.1021/jacs.3c01033
J. Am. Chem. Soc. 2023, 145, 6562–6576

utilizing as low as 5 mol % of neutral amine ligand Me_6Tren as the catalyst (Figure 9d).

This work unlocks new chemical space by proving the concept that, by tuning the chemical environments of organo-alkali metal complexes, it is possible to lead to diversified and divergent reaction patterns depending on the metal identity and aggregate size. Further work is underway in our groups in four directions: (1) Comprehensively explore the similarities and differences in reaction patterns between **1**-Li and **1**-Na and thoroughly understand their mechanisms; (2) push the strategy into heavier Group-1 metal congeners, i.e., organo-potassium, organorubidium, and organocesium; (3) exploit the ligand-catalysis strategy by employing more catalysts, such as bidentate tetramethylethylenediamine (TMEDA)[107] and *hexa*-dentate *N,N′,N″*-tris-(2-*N*-diethylaminoethyl)-1,4,7-triaza-cyclononane (DETAN),[108−110] and establish catalyst structure-reactivity-selectivity relationships; and (4) expand the methodology from methylenation ($C{=}CH_2$ bond formation) into general olefination ($C{=}CRR'$ bond formation, where R and R′ are H, aryls, or alkyls) and systematically study the *E*/*Z* selectivity.

■ ASSOCIATED CONTENT

Supporting Information

The Supporting Information is available free of charge at https://pubs.acs.org/doi/10.1021/jacs.3c01033.

Synthesis details, NMR spectra, and crystallographic and computational details (PDF)

Accession Codes

CCDC 2217099 (**1**-Na), 2217100 ($[NaCH_2SiMe_3]_\infty$), 2217101 (**5**), 2217102 (**3**-Na) and 2238438 (**6**) contain the supplementary crystallographic data for the corresponding complexes. These data can be obtained free of charge via www.ccdc.cam.ac.uk/data_request/cif, or by emailing data_request@ccdc.cam.ac.uk, or by contacting The Cambridge Crystallographic Data Centre, 12 Union Road, Cambridge CB2 1EZ, UK; fax: +441223 336033.

■ AUTHOR INFORMATION

Corresponding Authors

Claire L. McMullin − *Department of Chemistry, University of Bath, Bath BA2 7AY, U.K.*; orcid.org/0000-0002-4924-2890; Email: cm2025@bath.ac.uk

‖**Erli Lu** − *Chemistry−School of Natural and Environmental Sciences, Newcastle University, Newcastle upon Tyne NE1 7RU, U.K.*; orcid.org/0000-0002-0619-5967; Email: Erli.Lu@newcastle.ac.uk

Authors

Nathan Davison − *Chemistry−School of Natural and Environmental Sciences, Newcastle University, Newcastle upon Tyne NE1 7RU, U.K.*

Lu Zhang − *School of Mathematics and Physics, University of Science and Technology Beijing, Beijing 100083, P. R. China*

Shu-Xian Hu − *School of Mathematics and Physics, University of Science and Technology Beijing, Beijing 100083, P. R. China*; orcid.org/0000-0003-0127-3353

Paul G. Waddell − *Chemistry−School of Natural and Environmental Sciences, Newcastle University, Newcastle upon Tyne NE1 7RU, U.K.*

Corinne Wills − *Chemistry−School of Natural and Environmental Sciences, Newcastle University, Newcastle upon Tyne NE1 7RU, U.K.*

Casey Dixon − *Chemistry−School of Natural and Environmental Sciences, Newcastle University, Newcastle upon Tyne NE1 7RU, U.K.*

Complete contact information is available at: https://pubs.acs.org/10.1021/jacs.3c01033

Funding

E.L. thanks the Newcastle University Academic Track (NUAcT) Fellowship Scheme, EPSRC North East Centre of Energy Materials (NECEM) and the Royal Society of Chemistry Research Enablement Grants (E20-5153) for financial support. N.D. thanks Newcastle University for a NUAcT PhD studentship and the Royal Society of Chemistry Research Enablement Grants (E22-3348740748). C.L.M. thanks the University of Bath for access to Anatra High Performance Computing Service. S.-X.H. acknowledges the financial support from the National Natural Science Foundation of China (Nos. 21976014 and U1930402) and the generous grants of computer time from Tianhe2-JK.

Notes

The authors declare no competing financial interest.

‖Lead author.

■ ACKNOWLEDGMENTS

This article is dedicated to Professor Robert E. Mulvey, University of Strathclyde, for his pioneering contribution in Group-1 metal chemistry. The authors thank the Newcastle University Chemistry Technical Support Team (Dr. Laura McCorkindale, Dr. Amy Roberts and Mr. Niall Straughan) for supporting our research. E.L. thanks Drs. Keith Izod, Roly Armstrong, and Matthew Hopkinson (all at Newcastle University) for insightful discussions. The authors thank Professor Eva Hevia (Universität Bern) for providing in-depth insight of the recent publication[50] regarding **1**-Na from her group.

■ REFERENCES

(1) Wanklyn, J. A. XXII. On some new ethyl-compounds containing the alkali metals. *Proc. R. Soc. London* **1858**, *9*, 341−345.

(2) Seyferth, D. Alkyl and Aryl Derivatives of the Alkali Metals: Useful Synthetic Reagents as Strong Bases and Potent Nucleophiles. 1. Conversion of Organic Halides to Organoalkali-Metal Compounds. *Organometallics* **2006**, *25*, 2−24.

(3) Barluenga, J.; Fananás, F. J.; Yus, M. *β*-Substituted Organosodium and Organopotassium Compounds. Preparation and Characterization. *J. Org. Chem.* **1981**, *46*, 1281−1283.

(4) Schümann, U.; Behrens, U.; Weiss, E. Synthesis and Structure of a Phenylsodium Solvate, Bis[*μ*-phenyl-(pentamethyldiethylenetriamine)sodium]. *Angew. Chem., Int. Ed.* **1989**, *28*, 476−477.

(5) Corbelin, S.; Lorenzen, N. P.; Kopf, J.; Weiss, E. Über Metallalkyl- und Aryl-Verbindungen: Organonatrium-Verbindungen mit Benzyl-, Xylyl-, Diphenylmethyl- und 1-Phenyl-Ethyl-Carbanionen. *J. Organomet. Chem.* **1991**, *415*, 293−313.

(6) Corbelin, S.; Kopf, J.; Weiss, E. Über Metallalkyl- und -arylverbindungen, 48 Monomeres, tetrameres und polymeres Natriumfluorenid S [S = $Me_2N(CH_2)_2N(Me)(CH_2)_2NMe_2$, $Me_2N(CH_2)_nNMe_2$ (*n* = 2, 3)]. *Chem. Ber.* **1991**, *124*, 2417−2422.

(7) Viebrock, H.; Behrens, U.; Weiss, E. Über Metallalkyl- und -aryl-Verbindungen, 53. Synthese und Struktur von [9,10-Dihydroanthracenylnatrium(tmeda)]n und [9,10-

Dihydroanthracenylnatrium(pmdta)] (tmeda = Tetramethylethylendiamin, pmdta = Pentamethyldiethylentriamin). *Chem. Ber.* **1994**, *127*, 1399−1400.
(8) Jordan, V.; Behrens, U.; Olbrich, F.; Weiss, E. Über metallalkyl- und arylverbindungen LV. Cyclopentadienyl- und indenyl-verbindungen des kaliums und natriums. *J. Organomet. Chem.* **1996**, *517*, 81−88.
(9) den Besten, R.; Lakin, M. T.; Veldman, N.; Spek, A. L.; Brandsman, L. The Solid state structures of *ortho-β-*(*N,N*-dimethylamino) ethoxybenzene and the corresponding sodium compound: a new type of organolithium tetramer and a first example of an organosodium hexamer. *J. Organomet. Chem.* **1996**, *514*, 191−196.
(10) Eaborn, C.; Clegg, W.; Hitchcock, P. B.; Hopman, M.; Izod, K.; O'shaughnessy, P. N.; Smith, J. D. Organometallic Compounds of the Alkali Metals with Phenylsilyl Substituents at the Carbanionic Center. Crystal Structures of $LiC(SiMe_3)_2(SiMe_2Ph)\cdot Et_2O$, $NaC(SiMe_3)_2(SiMe_2Ph)\cdot$TMEDA, $NaC(SiMe_3)(SiMe_2Ph)_2\cdot$TMEDA, $\{LiCH(SiMe_2Ph)_2\}_2$, $RbC(SiMe_2Ph)_3$, and $CsC(SiMe_2Ph)_3$ (TMEDA = Tetramethylethylenediamine). *Organometallics* **1997**, *16*, 4728−4736.
(11) Gupta, S. K.; Kelkar, A. Synthesis and spectroscopic properties of alkali metal derivatives of tris{(diphenylphosphino)dimethylsilyl} methane. *Main Group Chem.* **2005**, *4*, 201−207.
(12) McMillen, C. H.; Gren, C. K.; Hanusa, T. P.; Rheingold, A. L. A tetrameric allyl complex of sodium, and computational modeling of the 23Na-allyl chemical shift. *Inorg. Chim. Acta* **2010**, *364*, 61−68.
(13) Clegg, W.; Conway, B.; Kennedy, A. R.; Klett, J.; Mulvey, R. E.; Russo, L. Synthesis and Structures of [(Trimethylsilyl)methyl]sodium and -potassium with Bi- and Tridentate N-Donor Ligands. *Eur. J. Inorg. Chem.* **2011**, 721−726.
(14) Baillie, S. E.; Clegg, W.; García-Álvarez, P.; Hevia, E.; Kennedy, A. R.; Klett, J.; Russo, L. Synthesis and characterization of an infinite sheet of metal−alkyl bonds: unfolding the elusive structure of an unsolvated alkali-metal trisalkylmagnesiate. *Chem. Commun.* **2011**, *47*, 388−390.
(15) Davidson, M. G.; Garcia-Vivo, D.; Kennedy, A. R.; Mulvey, R. E.; Robertson, S. D. Exploiting σ/π Coordination Isomerism to Prepare Homologous Organoalkali Metal (Li, Na, K) Monomers with Identical Ligand Sets. *Chem. − Eur. J.* **2011**, *17*, 3364−3369.
(16) Li, H.; Aquino, A. J. A.; Cordes, D. B.; Hung-Low, F.; Hase, W. L.; Krempner, C. A Zwitterionic Carbanion Frustrated by Boranes − Dihydrogen Cleavage with Weak Lewis Acids via an "Inverse" Frustrated Lewis Pair Approach. *J. Am. Chem. Soc.* **2013**, *135*, 16066−16069.
(17) Klett, J. Monometalated tribenzotriquinacene: *exo* and *endo* coordination of sodium and potassium with a rigid bowl-shaped hydrocarbon anion. *Chem. Commun.* **2014**, *50*, 7929−7932.
(18) von Pilgrim, M.; Mondeshki, M.; Klett, J. [Bis(Trimethylsilyl)-Methyl]Lithium and -Sodium: Solubility in Alkanes and Complexes with O- and N-Donor Ligands. *Inorganics* **2017**, *5*, 39.
(19) Vrána, J.; Jambor, R.; Růžička, A.; Dostál, L. New synthetic strategies leading to [RNPNR]− anions and the isolation of the $[P(Nt\text{-}Bu)_3]_3$− trianion. *Dalton Trans.* **2018**, *47*, 8434−8441.
(20) Tortajada, A.; Anderson, D. E.; Hevia, E. Gram-Scale Synthesis, Isolation and Characterisation of Sodium Organometallics: *n*BuNa and NaTMP. *Helv. Chim. Acta* **2022**, *105*, No. e202200060.
(21) Rae, A.; Byrne, K. M.; Brown, S. A.; Kennedy, A. R.; Krämer, T.; Mulvey, R. E.; Robertson, S. D. Sigma/pi Bonding Preferences of Solvated Alkali-Metal Cations to Ditopic Arylmethyl Anions. *Chem. − Eur. J.* **2022**, *28*, No. e202104260.
(22) Morantz, D. J.; Warhurst, E. The Reactions of Organic Halides with Organosodium Complexes in Solution. *Trans. Faraday Soc.* **1955**, *51*, 1375−1386.
(23) Benkeser, R. A.; Foster, D. J.; Sauve, D. M.; Nobis, J. F. Metalations with Organosodium Compounds. *Chem. Rev.* **1957**, *57*, 867−894.
(24) Gissot, A.; Becht, J.-M.; Desmurs, J. R.; Pévère, V.; Wagner, A.; Mioskowski, C. Directed *ortho*-Metalation, a New Insight into Organosodium Chemistry. *Angew. Chem., Int. Ed.* **2002**, *41*, 340−343.
(25) Weidmann, N.; Ketels, M.; Knochel, P. Sodiation of Arenes and Heteroarenes in Continuous Flow. *Angew. Chem., Int. Ed.* **2018**, *57*, 10748−10751.
(26) Colella, M.; Nagaki, A.; Luisi, R. Flow Technology for the Genesis and Use of (Highly) Reactive Organometallic Reagents. *Chem. − Eur. J.* **2020**, *26*, 19−32.
(27) Owen, D. W.; Poller, R. C. The Use of Organosodium Intermediates in the Synthesis of Alkyltin Chlorides. *J. Organomet. Chem.* **1983**, *255*, 173−178.
(28) Gulino, D.; Golé, J.; Pascault, J. P. Polymerisation anionique de l'acroleine—I. Polymerisations amorcees par des organo-sodiques dans le tetrahydrofuranne. *Eur. Polym. J.* **1979**, *15*, 469−475.
(29) Litvinenko, G. I.; Glazunova, E. V.; Arest-Yakubovich, A. A.; Basova, R. V.; Izyumnikov, A. L.; Rogozhkina, E. D. Sodium-initiated copolymerization of styrene and butadiene in hydrocarbon medium. *Vysokomolekulyarnye Soedineniya Seriya A & Seriya B* **1993**, *35*, A248−A254.
(30) Pakuro, N. I.; Arest-Yakubovich, A. A.; Rogozhkina, E. D.; Izyumnikov, A. L. Chain-breaking reactions in the course of isoprene polymerization with organosodium initiators. *Vysokomolekulyarnye Soedineniya Seriya A & Seriya B* **1994**, *36*, 136−139.
(31) Arest-Yakubovich, A. A.; Pakuro, N. I.; Zolotareva, I. V.; Kristal'nyl, E. V.; Basova, R. V. Polymerization of conjugated dienes initiated by soluble organosodium compounds in hydrocarbon solvents. *Polym. Int.* **1995**, *37*, 168−169.
(32) Shcheglova, L. V.; Pakuro, N. I.; Arest-Yakubovich, A. A. Kinetics of isoprene polymerization in the presence of 2-ethylhexylsodium and its mixtures with 2-ethylhexyllithium in hydrocarbon solvents. *Macrocol. Chem. Phys.* **1998**, *199*, 1025−1028.
(33) Inoue, T.; Yamamoto, S.; Sakagami, Y.; Horie, M.; Okano, K.; Mori, A. Cross-Coupling Polymerization of Organosodium for Polythiophene Synthesis. *Organometallics* **2021**, *40*, 3506−3510.
(34) Schlenk, W.; Holtz, J. The simplest organo-metallic alkali compounds. *Ber. Dtsch. Chem. Ges.* **1917**, *50*, 262−274.
(35) Wietelmann, U.; Klett, J. 200 Years of Lithium and 100 Years of Organolithium Chemistry. *Z. Anorg. Allg. Chem.* **2018**, *644*, 194−204.
(36) Rappoport, Z.; Mare, I. *The chemistry of organolithium compounds*; John Wiley & Sons, Ltd, 2004.
(37) Capriati, V.; Perna, F. M.; Salomone, A. "The Great Beauty" of organolithium chemistry: a land still worth exploring. *Dalton Trans.* **2014**, *43*, 14204−14210.
(38) Reich, H. J. Roles of Organolithium Aggregates and Mixed Aggregates in Organolithium Mechanisms. *Chem. Rev.* **2013**, *113*, 7130−7178.
(39) Harrison-Marchand, A.; Mongin, F. Mixed AggregAte (MAA): A Single Concept for All Dipolar Organometallic Aggregates. 1. Structural Data. *Chem. Rev.* **2013**, *113*, 7470−7562.
(40) Mongin, F.; Harrison-Marchand, A. Mixed AggregAte (MAA): A Single Concept for All Dipolar Organometallic Aggregates. 2. Syntheses and Reactivityies of Homo/HeteroMAAs. *Chem. Rev.* **2013**, *113*, 7563−7727.
(41) Haynes, W. M. Abundance of elements in the earth's crust and in the sea. In *CRC Handbook of Chemistry and Physics*, 97th ed.; CRC Press, 2017, pp 14−17.
(42) Aral, H.; Vecchio-Sadus, A. Toxicity of lithium to humans and the environment - A literature review. *Ecotoxicol. Environ. Saf.* **2008**, *70*, 349−356.
(43) Scott, A. Challenging China's dominance in the lithium market. *Chem. Eng. News* **2022**, *100* (38) https://cen.acs.org/energy/energy-storage-/Challenging-Chinas-dominance-lithium-market/100/i38.
(44) Asako, S.; Nakajima, H.; Takai, K. Organosodium compounds for catalytic cross-coupling. *Nat. Catal.* **2019**, *2*, 297−303.
(45) Wong, H. N. C. Is sodium finally coming of age? *Nat. Catal.* **2019**, *2*, 282−283.
(46) Asako, S.; Takahashi, I.; Nakajima, H.; Ilies, L.; Takai, K. Halogen−sodium exchange enables efficient access to organosodium compounds. *Commun. Chem.* **2021**, *4*, 76.
(47) Davey, S. G. Exchange made easy. *Nat. Rev. Chem.* **2021**, *5*, 368.

https://doi.org/10.1021/jacs.3c01033
J. Am. Chem. Soc. 2023, 145, 6562−6576

(48) Harenberg, J. H.; Annapureddy, R. R.; Karaghiosoff, K.; Knochel, P. Continuous Flow Preparation of Benzylic Sodium Organometallics. *Angew. Chem., Int. Ed.* **2022**, *61*, No. e202203807.
(49) Hazra, S.; Johansson Seechurn, C. C. C.; Handa, S.; Colacot, T. J. The Resurrection of Murahashi Coupling after Four Decades. *ACS Catal.* **2021**, *11*, 13188−13202.
(50) Anderson, D. E.; Tortajada, A.; Hevia, E. Highly Reactive Hydrocarbon Soluble Alkylsodium Reagents for Benzylic Aroylation of Toluenes using Weinreb Amides. *Angew. Chem., Int. Ed.* **2023**, No. e202218498.
(51) Davison, N.; Waddell, P. G.; Dixon, C.; Wills, C.; Penfold, T. J.; Lu, E. A monomeric (trimethylsilyl)methyl lithium complex: synthesis, structure, decomposition and preliminary reactivity studies. *Dalton Trans.* **2022**, *51*, 10707−10713.
(52) Lochmann, L.; Pospíšil, L. J.; Lím, D. On the interaction of organolithium compounds with sodium and potassium alkoxides. A new method for the synthesis of organosodium and organopotassium compounds. *Tetrahedron Lett.* **1966**, *7*, 257−262.
(53) Schlosser, M. Zur Aktivierung lithiumorganischer Reagenzien. *J. Organomet. Chem.* **1967**, *8*, 9−16.
(54) Two recent examples of the LIC-KOR superbases and their applications are: (a) Kim, D.; Lee, H.-J.; Shimizu, Y.; Yoshida, J.-I.; Kim, H. Direct C−H metalation of tetrahydrofuran and application in flow. *Nat. Synth.* **2022**, *1*, 558−564. (b) Benrath, P.; Kaiser, M.; Limbach, T.; Mondeshki, M.; Klett, J. Combining Neopentyllithium with Potassium tert-Butoxide: Formation of an Alkane-Soluble Lochmann−Schlosser Superbase. *Angew. Chem., Int. Ed.* **2016**, *55*, 10886−10889.
(55) Lochmann, L. Reaction of Organolithium Compounds with Alkali Metal Alkoxides − A Route to Superbases. *Eur. J. Inorg. Chem.* **2000**, *2000*, 1115−1126.
(56) Robertson, S. D.; Uzelac, M.; Mulvey, R. E. Alkali-Metal-Mediated Synergistic Effects in Polar Main Group Organometallic Chemistry. *Chem. Rev.* **2019**, *119*, 8332−8405.
(57) Bole, L. J.; Hevia, E. Activation of polar organometallic reagents with alkali-metal alkoxides. *Nat. Synth.* **2022**, *1*, 195−202.
(58) The $[NaCH_2SiMe_3]_\infty$ starting material was prepared following ref 13. We found that the $[NaCH_2SiMe_3]_\infty$ is more thermally stable than originally reported in ref 13 : the white crystalline solid was dissolved in C6D6 at 60 °C for several hours without NMR-observable decomposition. Slowly cooling the solution to room temperature resulted in crystals, which was subjected to SCXRD study and turned out to be a new polymorphous of $[NaCH_2SiMe_3]_\infty$ (CCDC 2217100). See Supporting Information for the SCXRD structures and more details.
(59) See Supporting Information for details.
(60) Lynch, J. R.; Kennedy, A. R.; Barker, J.; Reid, J.; Mulvey, R. E. Crystallographic Characterisation of Organolithium and Organomagnesium Intermediates in Reactions of Aldehydes and Ketones. *Helv. Chim. Acta* **2022**, *105*, No. e202200082.
(61) Hevia, E.; Honeyman, G. W.; Kennedy, A. R.; Mulvey, R. E. Trapping, Stabilization, and Characterization of an Enolate Anion of a 1,6-Adduct of Benzophenone Chelated by a Sodium Alkylamidozincate Cation. *J. Am. Chem. Soc.* **2005**, *127*, 13106−13107.
(62) Marchois, J.; Fressigné, C.; Lecachey, B.; Maddaluno, J. Base or nucleophile? DFT finally elucidates the origin of the selectivity between the competitive reactions triggered by MeLi or LDA on propanal. *Chem. Commun.* **2015**, *51*, 9801−9804.
(63) Mills, D. P.; Soutar, L.; Lewis, W.; Blake, A. J.; Liddle, S. T. Regioselective C−H Activation and Sequential C−C and C−O Bond Formation Reactions of Aryl Ketones Promoted by an Yttrium Carbene. *J. Am. Chem. Soc.* **2010**, *132*, 14379−14381.
(64) Tebbe, F. N.; Parshall, G. W.; Reddy, G. S. Olefin homologation with titanium methylene compounds. *J. Am. Chem. Soc.* **1978**, *100*, 3611−3613.
(65) Wittig, G.; Schöllkopf, U. Über Triphenyl-phosphin-methylene als olefinbildende Reagenzien I. Mitteil. *Chem. Ber.* **1954**, *87*, 1318−1330.
(66) Wittig, G.; Haag, W. Über Triphenyl-phosphinmethylene als olefinbildende Reagenzien II. Mitteil.1. *Chem. Ber.* **1955**, *88*, 1654−1666.
(67) Lin, W.-B.; Wilson, S. R.; Girolami, G. S. A Reversible Silicon-Carbon Bond Cleavage Process. Dynamics and Reactivity of Cp*2Ru2(μ-CH2)(SiMe3)(μ-Cl). *Organometallics* **1994**, *13*, 2309−2319.
(68) Peterson, D. J. Carbonyl olefination reaction using silylsubstituted organometallic compounds. *J. Org. Chem.* **1968**, *33*, 780−784.
(69) van Staden, L. F.; Gravestock, D.; Ager, D. J. New developments in the Peterson olefination reaction. *Chem. Soc. Rev.* **2002**, *31*, 195−200.
(70) Britten, T. K.; McLaughlin, M. G. Brønsted Acid Catalyzed Peterson Olefinations. *J. Org. Chem.* **2020**, *85*, 301−305.
(71) Johnson, C. R.; Tait, B. D. A Cerium(III) Modification of the Peterson Reaction: Methylenation of Readily Enolizable Carbonyl Compounds. *J. Org. Chem.* **1987**, *52*, 281−283.
(72) Mudryk, B.; Cohen, T. Generation, Some Synthetic Uses, and 1,2-Vinyl Rearrangements of Secondary and Tertiary Homoallyllithiums, Including Ring Contractions and A Ring Expansion. Remarkable Acceleration of the Rearrangement by an Oxyanionic Group. *J. Am. Chem. Soc.* **1993**, *115*, 3855−3865.
(73) Chen, F.; Mudryk, B.; Cohen, T. Generation, Rearrangements and Some Synthetic Uses of Bishomoallyllithiums. *Tetrahedron* **1994**, *50*, 12793−12810.
(74) Michler, W. Synthese aromatischer Ketone mittelst Chlorkohlenoxyd. *Ber. Deut. Chem. Ges.* **1876**, *9*, 716−718.
(75) Wu, S.; Yin, G.; Cheng, C.; Liang, B.; Zhang, H. Nucleophilic Substitution Reaction of Pentafluorophenyl Aminated Perylene Diimidesystem with *N,N*-Dimethylformamide. *Asia J. Org. Chem.* **2020**, *9*, 1076−1080.
(76) Golf, H. R. A.; Reissig, H.-U.; Wiehe, A. Nucleophilic Substitution on (Pentafluorophenyl)dipyrromethane: A New Route to Building Blocks for Functionalized BODIPYs and Tetrapyrroles. *Org. Lett.* **2015**, *17*, 982−985.
(77) Wilson, A. S. S.; Hill, M. S.; Mahon, M. F.; Dinoi, C.; Maron, L. Organocalcium-mediated nucleophilic alkylation of benzene. *Science* **2017**, *358*, 1168−1171.
(78) Qu, Z.-W.; Zhu, H.; Streubel, R.; Grimme, S. Organo-Group 2 Metal-Mediated Nucleophilic Alkylation of Benzene: Crucial Role of Strong Cation−π Interaction. *ACS Catal.* **2023**, *13*, 1686−1692.
(79) Chen, J.-H.; Lim, J. W.; Ong, D. Y.; Chiba, S. Iterative addition of carbon nucleophiles to N,N dialkyl carboxamides for synthesis of α-tertiary amines. *Chem. Sci.* **2021**, *13*, 99−104.
(80) Chen, H.; Huang, Y.-H.; Ye, J.-L.; Huang, P.-Q. Double Addition of Alkynyllithium Reagents to Amides/Lactams: A Direct and Flexible Synthesis of 3-Amino-1,4-diynes Bearing an Aza-Quaternary Carbon Center. *J. Org. Chem.* **2019**, *84*, 9270−9281.
(81) Verkruijsse, H. D.; Heus-Kloos, Y. A.; Brandsma, L. Efficient methods for the preparation of acetylenic ketones. *J. Organomet. Chem.* **1988**, *338*, 289−294.
(82) Olah, G. A.; Surya Prakash, G. K.; Arvanaghi, M. Synthetic Methods and Reactions; Part 109. Improved Preparation of Aldehydes and Ketones from *N,N'*-Dimethylamides and Grignard Reagents. *Synthesis* **1984**, 228−230.
(83) Ghinato, S.; Territo, D.; Maranzana, A.; Carpriati, V.; Blangetti, M.; Prandi, C. A Fast and General Route to Ketones from Amides and Organolithium Compounds under Aerobic Conditions: Synthetic and Mechanistic Aspects. *Chem. − Eur. J.* **2021**, *27*, 2868−2874.
(84) Ager, D. J. Reactions of Phenyllithiotrimethylsilylmethyllithium: Preparation of α-Phenyllithioketones and Additions to 2-Cyclohexen-1-one. *Tetrahedron Lett.* **1981**, *22*, 2803−2806.
(85) Inoue, H.; Nagata, T. Electron-transfer Reduction of Esters with Carbanions mediated by an Iron-Sulphur Cluster. *J. Chem. Soc., Chem. Commun.* **1986**, 1178−1179.
(86) Beak, P.; Brown, R. A. The Tertiary Amide as an Effective Director of Ortho Lithiation. *J. Org. Chem.* **1982**, *47*, 34−46.
(87) ACD-A: Sigma-Aldrich (Spectral data were obtained from Advanced Chemistry Development, Inc.)

https://doi.org/10.1021/jacs.3c01033
J. Am. Chem. Soc. 2023, 145, 6562−6576

(88) The BDE data source: (a) Cottrell, T. L. *The Strengths of Chemical Bonds*, 2nd ed.; Butterworth: London, 1958. (b) Darwent, B. *National Standard Reference Data Series*; National Bureau of Standards: Washington, no. 31, 1970. (c) Benson, S. W. Bond energies. *J. Chem. Educ.* **1965**, *42*, 502−518. (d) Kerr, J. A. Bond Dissociation Energies by Kinetic Methods. *Chem. Rev.* **1966**, *66*, 465−500.
(89) Kawashima, T.; Iwama, N.; Okazaki, R. Synthesis and x-ray crystallographic analysis of pentacoordinate 1,2-oxasiletanides, intermediates of the Peterson reaction. *J. Am. Chem. Soc.* **1992**, *114*, 7598−7599.
(90) Hermann, A.; Opper, U.; Voß, A.; Brieger, L.; Otte, F.; Unkelbach, C.; O'Shea, D. F.; Strohmann, C. Aminopotassiation by Mixed Potassium/Lithium Amides: A Synthetic Path to Difficult to Access Phenethylamine Derivates. *Angew. Chem., Int. Ed.* **2020**, *59*, 22500−22504.
(91) Wittig, G.; Haag, W. Über Triphenyl-phosphinmethylene als olefinbildende Reagenzien (II. Mitteil). *Chem. Ber.* **1955**, *88*, 1654−1666.
(92) Julia, M.; Paris, J.-M. Syntheses a l'aide de sulfones v(+)-methode de synthese generale de doubles liaisons. *Tetrahedron Lett.* **1973**, *14*, 4833−4836.
(93) Blakemore, P. R.; Cole, W. J.; Kocieński, P. J.; Morley, A. A Stereoselective Synthesis of trans-1,2-Disubstituted Alkenes Based on the Condensation of Aldehydes with Metallated 1-Phenyl-1H-tetrazol-5-yl Sulfones. *Synlett* **1998**, *1998*, 26−28.
(94) Kurogi, T.; Kamitani, M.; Manor, B. C.; Carroll, P. J.; Mindiola, D. J. Reactivity Studies of a Zirconium Methylidene Complex: Group Transfer and Methylenation Reactions. *Organometallics* **2017**, *36*, 74−79.
(95) Birkelbach, V. M.; Kracht, F.; Martin Dietrich, H.; Stuhl, C.; Maichle-Mössmer, C.; Anwander, R. A Rare-Earth-Metal Ensemble of the Tebbe Reagent: Scope of Coligands and Carbonyl Olefination. *Organometallics* **2020**, *39*, 3490−3504.
(96) Kauffmann, T.; Papenberg, M.; Wieschollek, R.; Sander, J. Organomolybdän- und Organowolfram-Reagenzien, II. über den carbonylolefinierenden μ-Methylenkomplex aus Mo2Cl10 und vier äquivalenten Methyllithium. *Chem. Ber.* **1992**, *125*, 143−148.
(97) Takai, N.; Nitta, K.; Utimoto, K. Simple and selective method for RCHO → (E)-RCH═CHX conversion by means of a CHX_3−$CrCl_2$ system. *J. Am. Chem. Soc.* **1986**, *108*, 7408−7410.
(98) Ahlberg, P.; Karlsson, A.; Davidsson, Ö.; Hilmersson, G.; Löwendahl, M. Mechanism and Solvent Catalysis of the Degenerate 1,12-Metalations of [1.1]Ferrocenophanyllithium and [1.1]-Ferrocenophanylsodium Studied by NMR Spectroscopy. *J. Am. Chem. Soc.* **1997**, *119*, 1751−1757.
(99) Eberhardt, G. G.; Butte, W. A. A Catalytic Telomerization Reaction of Ethylene with Aromatic Hydrocarbons. *J. Org. Chem.* **1964**, *29*, 2928−2932.
(100) Screttas, C. G.; Eastham, J. F. Alkyllithium-Amine Crystalline Complexes. *J. Am. Chem. Soc.* **1965**, *87*, 3276−3277.
(101) Trimitsis, G. B.; Tuncay, A.; Beyer, R. D. Metalations of Dimethylarenes with Organosodium Reagents. The Catalytic Effect of Certain Tertiary Amines. *J. Am. Chem. Soc.* **1972**, *94*, 2152−2153.
(102) Asano, Y.; Ilda, A.; Tomioka, K. The Chiral Ligand-Catalyzed Enantioselective Conjugate Addition of Organolithium to BHA Enoate. *Chem. Pharm. Bull.* **1998**, *46*, 184−186.
(103) Ramirez, A.; Sun, X.-F.; Collum, D. B. Lithium Diisopropylamide-Mediated Enolization: Catalysis by Hemilabile Ligands. *J. Am. Chem. Soc.* **2006**, *128*, 10326−10336.
(104) Ma, Y.; Woltornist, R. A.; Algera, R. F.; Collum, D. B. Reactions of Sodium Diisopropylamide: Liquid-Phase and Solid−Liquid Phase-Transfer Catalysis by *N*,*N*,*N*′,*N*″,*N*″-Pentamethyldiethylenetriamine. *J. Am. Chem. Soc.* **2021**, *143*, 13370−13381.
(105) Srinivasan, B. A guide to the Michaelis-Menten equation: steady state and beyond. *FEBS J.* **2022**, *289*, 6086−6098.
(106) Lehninger, A. L.; Nelson, D. L.; Cox, M. M. *Lehninger principles of biochemistry*; W.H. Freeman: New York, 2005.
(107) Collum, D. A. Is *N*,*N*,*N*′,*N*′-tetramethylethylenediamine a good ligand for lithium? *Acc. Chem. Res.* **1992**, *25*, 448−454.
(108) Davison, N.; Falbo, E.; Waddell, P. G.; Penfold, T. J.; Lu, E. A monomeric methyllithium complex: synthesis and structure. *Chem. Commun.* **2021**, *57*, 6205−6208.
(109) Davison, N.; Zhou, K.; Waddell, P. G.; Wills, C.; Dixon, C.; Hu, S.-X.; Lu, E. Versatile Coordination Modes of Multidentate Neutral Amine Ligands with Group 1 Metal Cations. *Inorg. Chem.* **2022**, *61*, 3674−3682.
(110) Davison, N.; Quirk, J. A.; Wills, C.; Dixon, C.; Waddell, P. G.; Dawson, J. A.; Lu, E. Elucidating Solution-State Coordination Modes of Multidentate Neutral Amine Ligands with Group-1 Metal Cations: Variable-Temperature NMR Studies. *Inorg. Chem.* **2022**, *61*, 15204−15212.

https://doi.org/10.1021/jacs.3c01033
J. Am. Chem. Soc. 2023, 145, 6562−6576